Supporting Information for

Flux Growth of High Entropy Layered Perovskite-type Oxysulfide $Gd_{2/3}Y_{1/3}Sm_{1/3}Tb_{1/3}Ho_{1/3}Ti_2O_5S_2$ Single Crystals

*Fumitaka Hayashi,[*a,b] Harumu Sugiyama,[c] Yuto Yokotsuka,[c] Makoto Nagasako,[d] Haruhiko Morito,[d] Tetsuya Yamada,[a,b] and Katsuya Teshima[*a,b]*

[a] Department of Materials Chemistry, Faculty of Engineering, Shinshu University, 4-17-1 Wakasato, Nagano 380-8553, Japan

[b] Institute for Aqua Regeneration, Shinshu University, 4-17-1 Wakasato, Nagano 380-8553, Japan

[c] Department of Science and Technology, Graduate School of Science and Technology, Shinshu University, 4-17-1 Wakasato, Nagano 380-8553, Japan

[d] Institute for Materials Research, Tohoku University, Katahira 2-1-1, Aoba-ku, Sendai, Miyagi 980-8577, Japan

* Corresponding author, fhayash@shinshu-u.ac.jp; teshima@shinshu-u.ac.jp

Table S1. Flux growth conditions for multicomponent GTOS single crystals

Run	Solute												Flux	
	Gd_2O_3	$(CH_3COO)_3Gd$	Y_2O_3	Sm_2O_3	$(CH_3COO)_3Tb$	Ho_2O_3	Dy_2O_3	Gd_2S_3	Y_2S_3	Sm_2S_3	Tb_2S_3	Ho_2S_3	LiCl	$CaCl_2$
	/ mmol	/ mmol	/ mmol	/ mmol	/ mmol	/ mmol	/ mmol	/ mmol	/ mmol	/ mmol	/ mmol	/ mmol	/mmol	/mmol
1	0.14	0	0.050	0.050	0.10	0.050	0	0.67	0	0	0	0	0	0
2	0.14	0	0	0.050	0.10	0.050	0.050	0.67	0	0	0	0	0	0
3	0.14	0	0.050	0.050	0	0.050	0.050	0.67	0	0	0	0	0	0
4	0.14	0	0.050	0.050	0.10	0	0.050	0.67	0	0	0	0	0	0
5	0.14	0	0.050	0	0.10	0.050	0.050	0.67	0	0	0	0	0	0
6	0.033	0	0.075	0.075	0.15	0.075	0	0.67	0	0	0	0	0	0
7	0	0	0.085	0.085	0.17	0.085	0	0.67	0	0	0	0	0	0
8	0	0.66	0	0	0	0	0	0.17	0.13	0.13	0.13	0.13	0	0
9	0	0.66	0	0	0	0	0	0.066	0.15	0.15	0.15	0.15	0	0
10	0	0.66	0	0	0	0	0	0	0.17	0.17	0.17	0.17	0	0
11	0	0	0.085	0.085	0.17	0.085	0	0.67	0	0	0	0	5.4	3.6
12	0	0.66	0	0	0	0	0	0.17	0.13	0.13	0.13	0.13	5.4	3.6
13	0	0.66	0	0	0	0	0	0.066	0.15	0.15	0.15	0.15	5.4	3.6
14	0	0.66	0	0	0	0	0	0	0.17	0.17	0.17	0.17	5.4	3.6

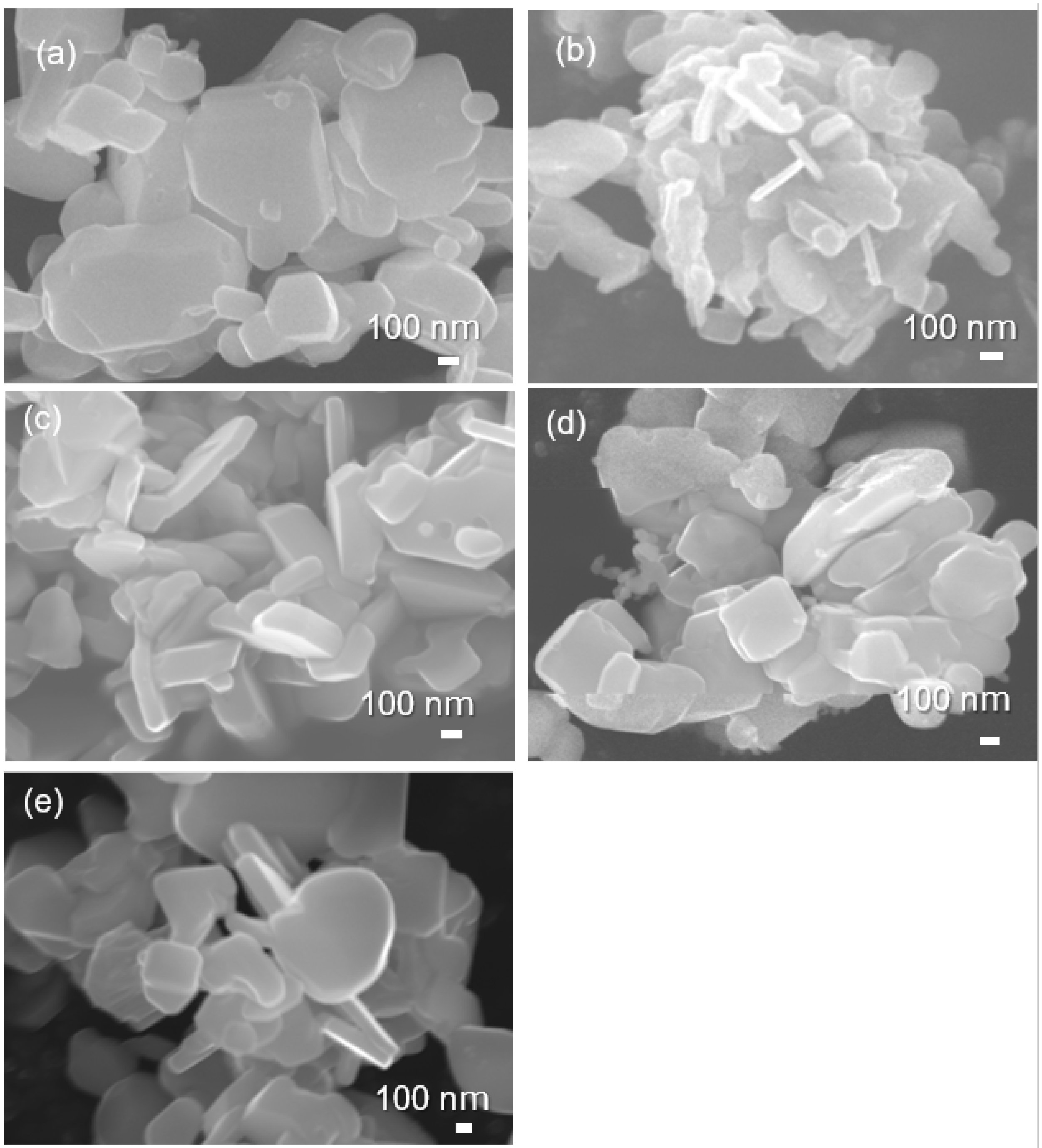

Figure S1. FE-SEM images of solid-state reaction (SSR) synthesized multicomponent GTOS (MGTOS) crystals: (a) $G_{1.6}Y_{0.1}Sm_{0.1}Tb_{0.1}Ho_{0.1}Ti_2O_5S_2$, (b) $G_{1.6}Sm_{0.1}Tb_{0.1}Dy_{0.1}Ho_{0.1}Ti_2O_5S_2$, (c) $G_{1.6}Y_{0.1}Sm_{0.1}Dy_{0.1}Ho_{0.1}Ti_2O_5S_2$, (d) $G_{1.6}Y_{0.1}Sm_{0.1}Tb_{0.1}Dy_{0.1}Ti_2O_5S_2$, and (e) $G_{1.6}Y_{0.1}Tb_{0.1}Dy_{0.1}Ho_{0.1}Ti_2O_5S_2$. The synthetic conditions are shown in Table S1, Runs 1-5.

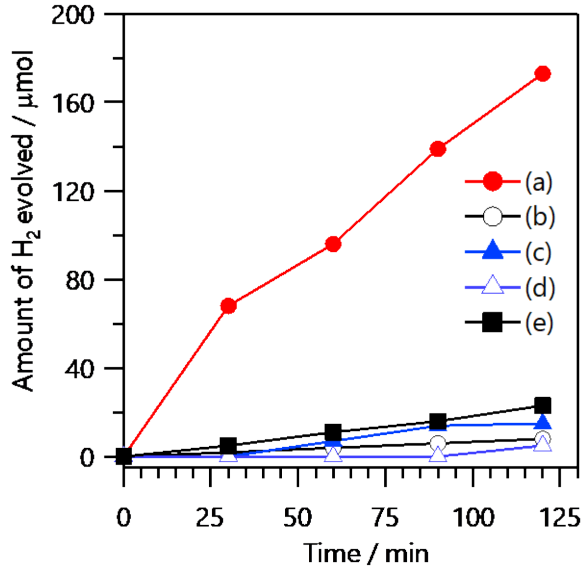

Figure S2. Time courses of H_2 evolution from (a) $Gd_{1.6}Y_{0.1}Sm_{0.1}Tb_{0.1}Ho_{0.1}Ti_2O_5S_2$, (b) $Gd_{1.6}Sm_{0.1}Tb_{0.1}Dy_{0.1}Ho_{0.1}Ti_2O_5S_2$, (c) $Gd_{1.6}Y_{0.1}Sm_{0.1}Dy_{0.1}Ho_{0.1}Ti_2O_5S_2$, (d) $Gd_{1.6}Y_{0.1}Sm_{0.1}Tb_{0.1}Dy_{0.1}Ti_2O_5S_2$, and (e) $Gd_{1.6}Y_{0.1}Tb_{0.1}Dy_{0.1}Ho_{0.1}Ti_2O_5S_2$. Condition: Cat., 200 mg; 0.5wt% Ir (MW), 1.0wt% Pt (MW), 0.5wt% CrO_x (PD); solution MeOH 150 mL, Current, 20 A Xe lamp; λ, > 420 nm CM1.

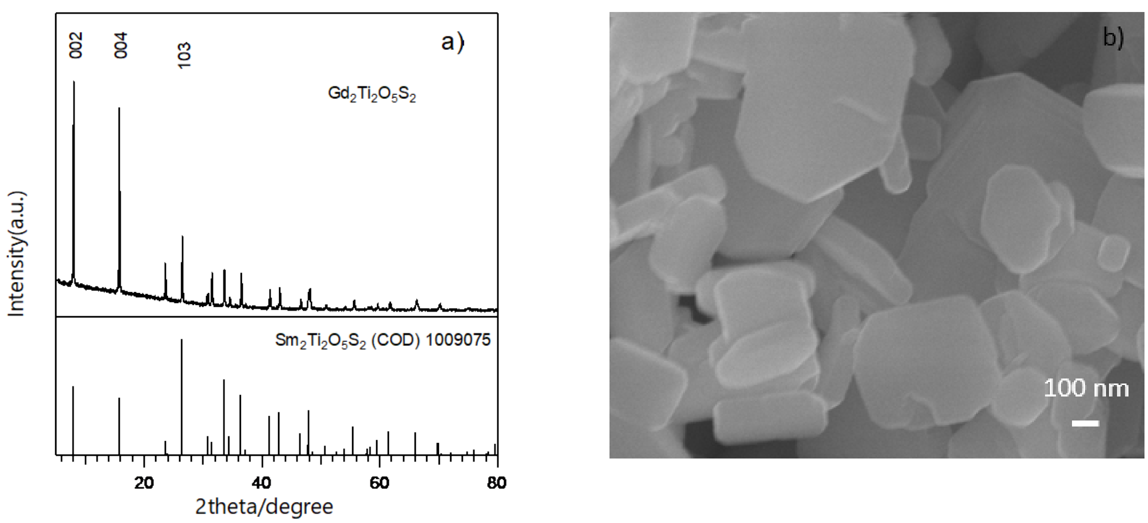

Figure S3. (a) XRD pattern and (b) SEM image of $Gd_2Ti_2O_5S_2$ crystals grown from a LiCl-$CaCl_2$ flux at 700 °C. Solute concentration is 10 mol %.

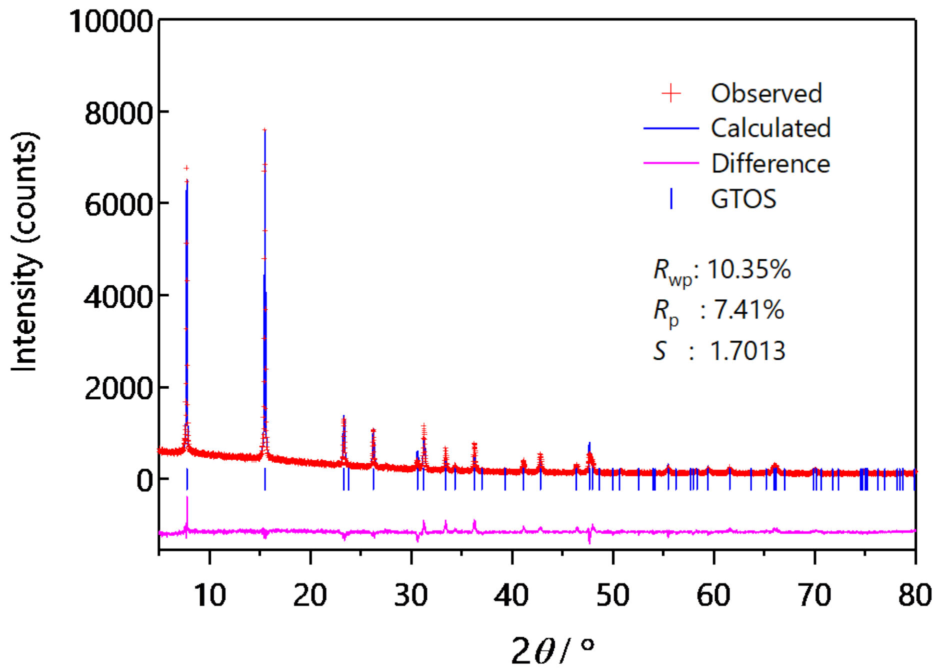

Figure S4. Rietveld analysis results obtained from the XRD pattern of $Gd_{0.66}Y_{0.33}Sm_{0.33}Tb_{0.33}Ho_{0.33}Ti_2O_5S_2$ crystal grown from a LiCl-$CaCl_2$ flux at 700 °C.

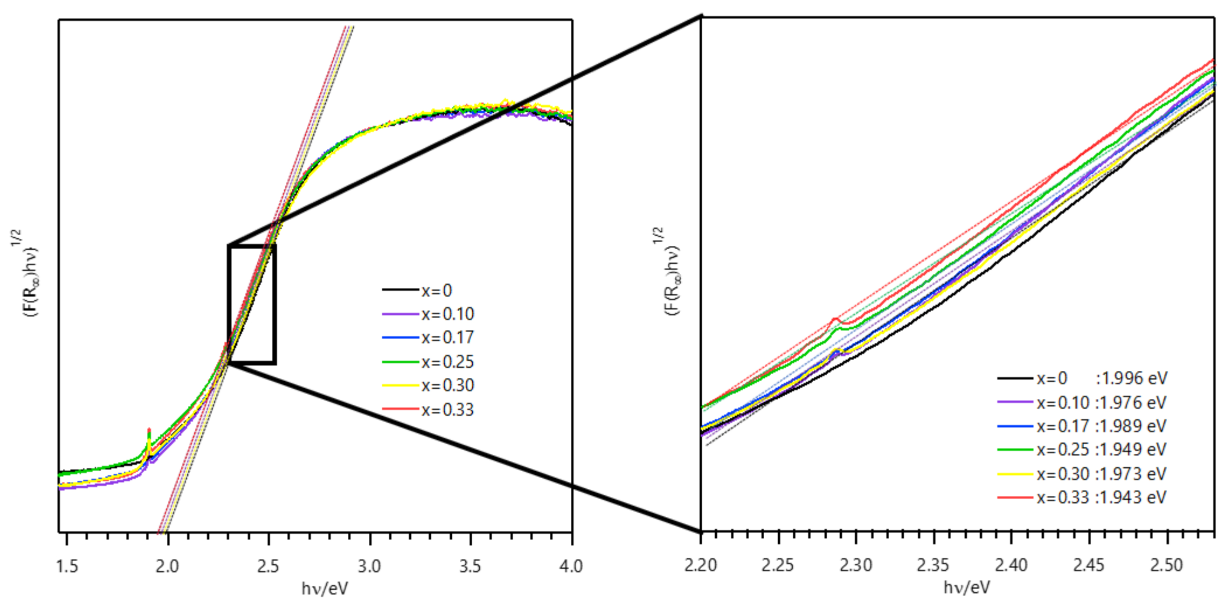

Figure S5. Tauc plot of MGTOS crystals prepared at 700 °C using (a) SSR and (b–f) flux growth at different solute concentrations of (b) 95 mol%, (c) 80 mol%, (d) 50 mol%, (e) 20 mol%, and (f) 10 mol%.

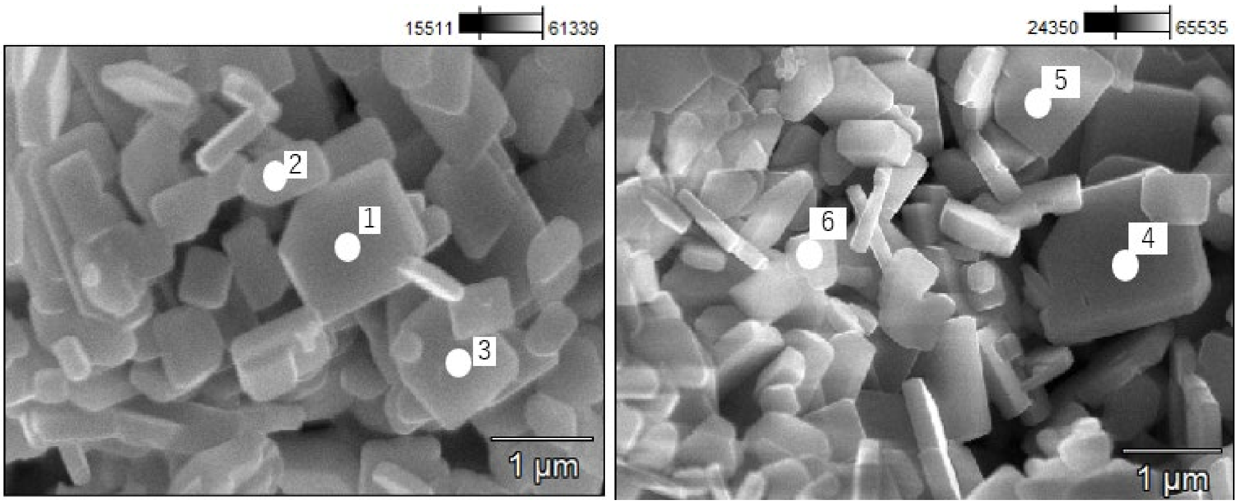

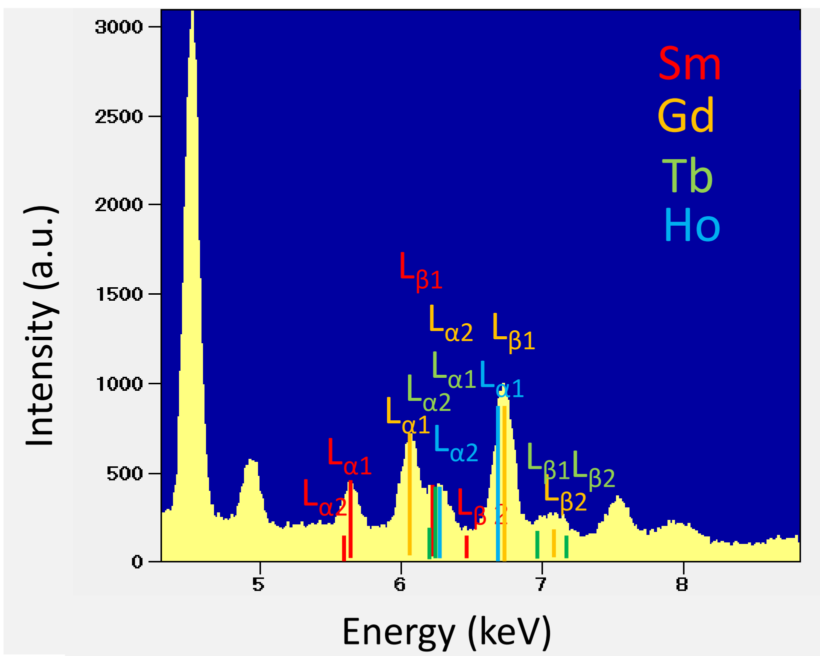

Point	Atomic ratio				
	Gd	Y	Sm	Tb	Ho
1	0.796	0.067	0.066	0.058	0.014
2	0.813	0.07	0.052	0.059	0.004
3	0.826	0.066	0.052	0.048	0.009
4	0.799	0.049	0.065	0.063	0.024
5	0.821	0.047	0.057	0.064	0.012
6	0.814	0.036	0.045	0.056	0.031
Average	0.812	0.056	0.056	0.058	0.016

Figure S6. (top) FE-SEM image and (middle) EDS spectrum, and (bottom) atomic ratio for rare-earth elements in the FE-SEM images on $Gd_{1.6}Y_{0.1}Sm_{0.1}Tb_{0.1}Ho_{0.1}Ti_2O_5S_2$ grown from a LiCl-$CaCl_2$ flux.

a)

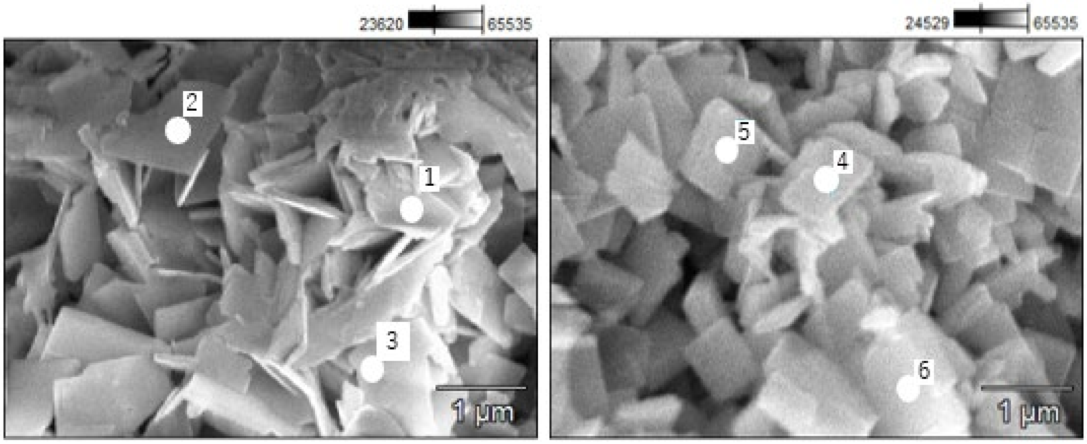

b)

Point	Atomic ratio				
	Gd	Y	Sm	Tb	Ho
1	0.329	0.250	0.182	0.137	0.102
2	0.367	0.276	0.145	0.125	0.087
3	0.385	0.232	0.150	0.119	0.114
4	0.307	0.253	0.186	0.124	0.130
5	0.342	0.254	0.180	0.101	0.123
6	0.315	0.233	0.181	0.126	0.145
Average	0.341	0.250	0.171	0.122	0.117

Figure S7. (a) FE-SEM image and (b) atomic ratio for rare-earth elements in the FE-SEM images on $Gd_{0.8}Y_{0.3}Sm_{0.3}Tb_{0.3}Ho_{0.3}Ti_2O_5S_2$ grown from a LiCl-$CaCl_2$ flux.

(a)

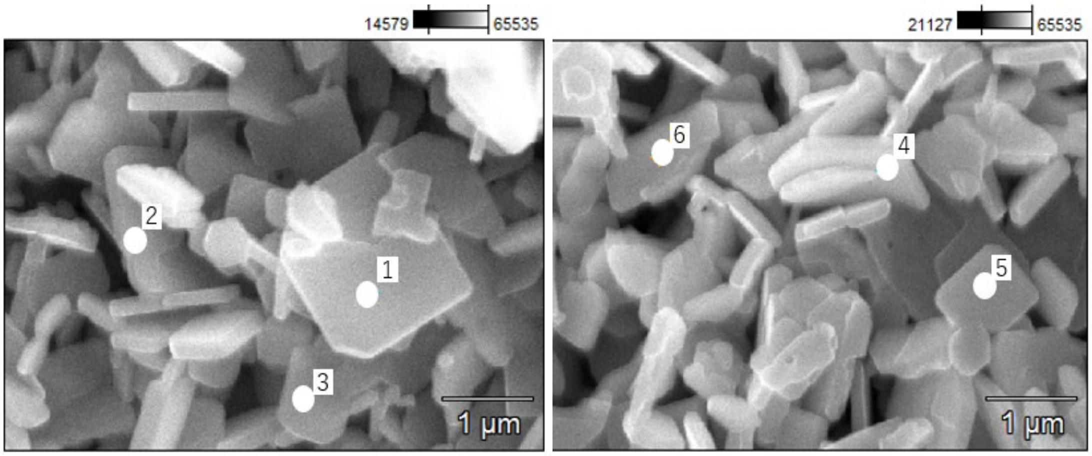

(b)

Point	Atomic ratio				
	Gd	Y	Sm	Tb	Ho
1	0.277	0.181	0.305	0.132	0.106
2	0.270	0.242	0.273	0.122	0.093
3	0.290	0.239	0.254	0.124	0.093
4	0.256	0.227	0.173	0.193	0.150
5	0.253	0.193	0.180	0.194	0.180
6	0.269	0.233	0.173	0.181	0.144
Average	0.269	0.219	0.226	0.158	0.128

Figure S8. (a) FE-SEM image and (b) the corresponding EDS mapping analysis result for $Gd_{0.67}Y_{0.33}Sm_{0.33}Tb_{0.33}Ho_{0.33}Ti_2O_5S_2$ grown from a LiCl-$CaCl_2$ flux.

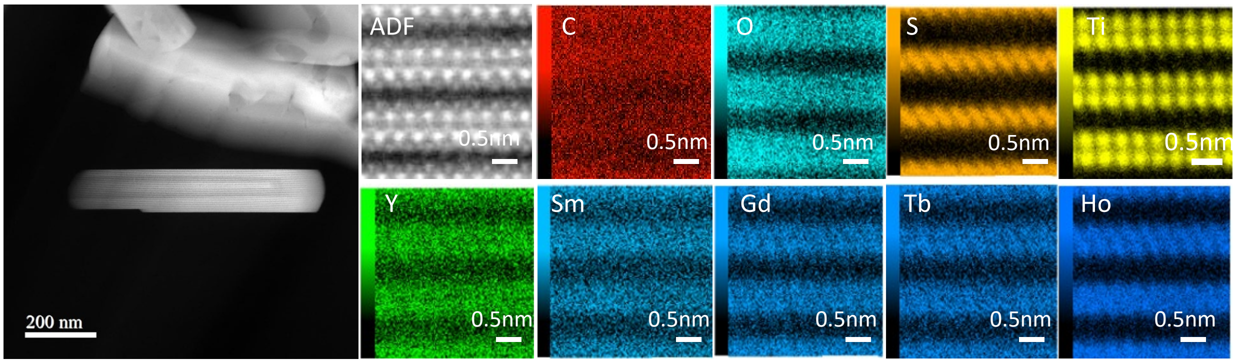

Figure S9. HAADF-STEM image with EDS elemental maps of $Gd_{0.67}Y_{0.33}Sm_{0.33}Tb_{0.33}Ho_{0.33}Ti_2O_5S_2$ grown from a LiCl-$CaCl_2$ flux, taken along the [100] direction.